Journal of Nuclear Materials 378 (2008) 40–44

Contents lists available at ScienceDirect

Journal of Nuclear Materials

journal homepage: www.elsevier.com/locate/jnucmat

Atomic diffusion mechanism of Xe in UO_2

Younsuk Yun [a,*], Hanchul Kim [b], Heemoon Kim [c], Kwangheon Park [d]

[a] Department of Physics and Materials Science, Box 530, Uppsala University, S-75121 Uppsala, Sweden
[b] Department of Physics, Sookmyung Women's University, Seoul 140-702, Republic of Korea
[c] Korea Atomic Energy Research Institute, P.O. Box 105, Yuseong, Daejeon 305-353, Republic of Korea
[d] Department of Nuclear Engineering, KyungHee University, Suwon 449-701, Republic of Korea

ARTICLE INFO

Article history:
Received 29 October 2007
Accepted 22 April 2008

PACS:
61.72.Ji
66.30.Jt

ABSTRACT

We have investigated vacancy-assisted diffusion of Xe in uranium dioxide (UO_2) calculating incorporation, binding, and migration energies. All the energy values have been obtained using the density functional theory (DFT) within the generalized gradient approximation (GGA) and the projector-augmented-wave (PAW) method. Considering spin-polarization effect, we find that the computed migration energy is reduced by and agrees well with experimental data compared to those obtained from non-magnetic calculations. We also find that an oxygen vacancy lowers the migration energy of a uranium vacancy by about 1 eV, enhancing an effective movement of vacancy clusters consisting of both uranium and oxygen vacancies. Furthermore, the strain energy of Xe is large enough to contribute to the clustering of vacancies making it the driving force for the vacancy-assisted diffusion of Xe in UO_2. In summary all the calculated results suggest that the trivacancy is a major diffusion pathway of Xe in UO_2.

1. Introduction

The atomic transport processes in UO_2 are of great interest for understanding UO_2's performance during irradiation. Particularly, the behavior of fission gases is an important performance-limiting factor since fission gas release increases the temperature due to a decrease in the thermal conductivity across the fuel clad gap, resulting in an increase of the fuel pressure. For these reasons, the diffusion characteristics of fission gases have been the subject of extensive research [1–4]. Lawrence [5] has reviewed data on gas diffusion in UO_2 and reported that the diffusion coefficient of fission gases is significantly affected by the defect structure of UO_2. The detailed lattice structural analysis done by Matzke et al. [6–8] reports the fission gas diffusion in UO_2 at low gas concentrations to proceed via an electrically neutral trivacancy that consists of a uranium vacancy and two oxygen vacancies. Recently, experimental methods using *in situ* TEM (transmission electron microscope) experiments [9] and PIXE (particle induced X-ray emission) measurements [10] have been used to investigate the location and diffusion of fission products such as Xe, He, and Nd.

Several theoretical methods have also been used to study the behavior of fission products in UO_2. Catlow et al. [11,12] and Grimes et al. [13–15] calculated incorporation and solution energies of Xe and He in UO_2 using the Mott–Littleton approximation with empirical potentials. *Ab initio* methods based on the DFT [16] have been successfully used since the mid-90's. Petit et al. [17] investigated the stability of Kr in UO_2 applying the linear muffin–tin orbital method in the atomic sphere approximation [18,19], and Crocombette [20] also calculated the energies of Kr, I, Cs, Sr, and He in UO_2. Recently, Freyss et al. [21] compared the volume variation induced by He and Xe, by using the pseudopotential and the GGA method [22].

Despite the large amount of work performed, the mechanisms of fission gas release in UO_2 are still not known. One reason for this may be large variation in experimental data for the diffusion coefficient and activation energy which make it extremely difficult to develop constant plausible models based on experimental observations. In addition to this, most of the previous studies concentrated on the stability of fission products, rather than on diffusion mechanism.

In this study, we therefore focus on studying the atomic diffusion mechanism of Xe, which is one of the highest fractional released fission gases in UO_2. The GGA-PAW method [23] is used to obtain energy values. In particular, we focus on the role of point defect, especially vacancy defects, which is thought to be a major diffusion channel for fission gases in the UO_2 matrix [7,15,17]. A larger supercell containing 96 atoms is employed to reduce any artificial error caused due to the use of a small supercell. First, we calculate the incorporation energy [15,20,21] of Xe located at different five vacancies. These are the uranium vacancy (V_U), oxygen vacancy (V_O), divacancy consisting of a uranium and an oxygen vacancy (V_{UO}), trivacancy (V_{UO_2}), and tetravacancy ($V_{U_2O_2}$). The stability of these vacancies as Xe sites are compared using the relative incorporation energies. Next, we calculate the movement of defect

* Corresponding author. Tel.: +46 18 471 7308; fax: +46 18 471 3524.
E-mail address: younsuk.yun@fysik.uu.se (Y. Yun).

0022-3115/$ - see front matter © 2008 Elsevier B.V. All rights reserved.
doi:10.1016/j.jnucmat.2008.04.013

elements and investigate the effect of the spin-polarization on the computed migration energies. Finally, we examine the diffusion mechanism of Xe with the effective movements of vacancies and predict a detailed diffusion process of Xe by a vacancy-assisted mechanism in the UO_2 lattice.

2. Calculation details

Fig. 1(a) and (b) show unitcell and a $2 \times 2 \times 2$ supercell of UO_2, respectively. The energy needed to incorporate a free Xe atom at an octahedral interstitial site (OIS) in UO_2 is calculated as shown

$$E^{I}_{Xe_{OIS}} = E^{N+1}_{Xe_{OIS}} - (E^{N}_{perfect} + E_{Xe_{free}}) \quad (1)$$

where $E^{N+1}_{Xe_{OIS}}$ is the total energy of a supercell containing Xe trapped at an OIS, and $E^{N}_{perfect}$ is the energy of a defect-free supercell. $E_{Xe_{free}}$ is the energy of free Xe atom and N is the number of atoms in a supercell. In this study, focus is on the relative incorporation energy of Xe between an OIS and other trap sites assuming that Xe exists in UO_2. We calculate the relative incorporation energies of Xe for five different trap sites: V_O, V_U, V_{UO}, V_{UO_2}, and $V_{U_2O_2}$ shown in Table 1.

Fig. 2 describes the details of calculating the relative incorporation energy. The system S_1 in Fig. 2 indicates two structures containing Xe_{OIS} and a V_Z which is a vacancy of the Z-element (Z= cation, anion, or their compounds), respectively. These two structures are far enough from each other to ignore the interaction between Xe_{OIS} and V_Z. S_2 consists of a perfect crystal and a Xe_Z-containing system.

The relative incorporation energy of Xe for an OIS and V_Z is calculated from the total energy difference between the S_1 and S_2 as follows:

$$E_I = E_{S_2} - E_{S_1} = (E^{N}_{perfect} + E^{N}_{Xe_Z}) - (E^{N+1}_{Xe_{OIS}} + E^{N-1}_{V_Z}) \quad (2)$$

We calculated the formation energies of the oxygen Frenkel pair and Schottky defects, respectively, as follows. These are known as the dominant intrinsic defects in UO_2

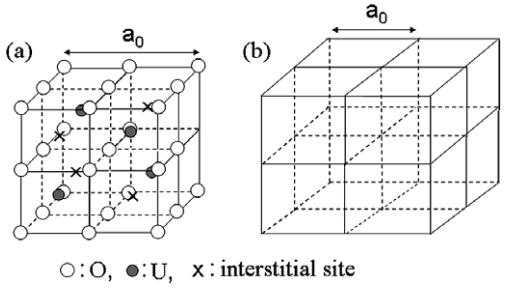

Fig. 1. (a) Conventional unitcell of UO_2. Oxygen atoms are located at the corners of small cubes, and uranium atoms are located at the center of an alternative cubes. × indicates the octahedral interstitial site in FCC structure. (b) A $2 \times 2 \times 2$ supercell of UO_2 containing 96 atoms used in the current study.

Table 1
Calculated incorporation energies of Xe for five different vacancies and OIS

Xe sites	OIS	V_O	V_U	V_{UO}	V_{UO_2}	$V_{U_2O_2}$
Incorporation energy (E^I) (eV)	1.43	−2.90	−6.83	−9.71	−10.97	−12.07
Formation energy (E^f_V) (eV)	0.00	1.84	3.27	4.71	6.44	8.13
$E^I + E^f_V$	1.43	−1.06	−3.56	−5.00	−4.52	−3.94

$E^f_{F_O} = 3.7(3.0\text{–}4.0)^*$, $E^f_S = 7.0(6.0\text{–}7.0)^*$.
The incorporation energy is increased as the size of vacancy. The formation energy of each vacancy is derived by using the thermodynamic relation between oxygen Frenkel pair and Schottky defects [13–15]. (* indicates the experimental data of the formation energies of oxygen Frenkel pair ($E^f_{F_O}$) and Schottky trio (E^f_S) defects [34]).

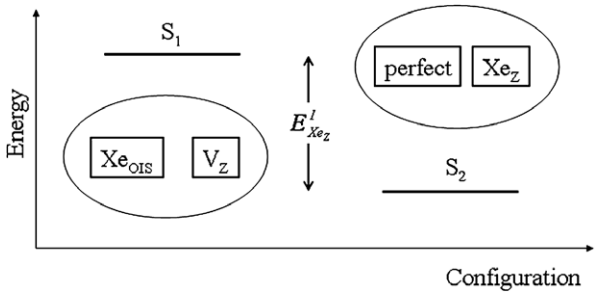

Fig. 2. Incorporation energy of Xe at a vacancy. The system S_1 contains Xe_{OIS} and V_Z: Xe is located at OIS and V_Z is a vacancy of Z-element which is uranium atom, oxygen atom, or their compounds. The S_2 contains Xe_Z that Xe trapped at V_Z. The incorporation energy of Xe for V_Z, $E^I_{Xe_Z}$, is calulated the energy difference between the S_1 and S_2.

$$E^f_{F_O} = E^{N-1}_{V_O} + E^{N+1}_{I_O} - 2 \times E^N \quad (3)$$

$$E^f_S = E^{N-1}_{V_U} + 2 \times E^{N-1}_{V_O} - 3 \times E^N + \mu_U + 2 \times \mu_O \quad (4)$$

$$= E^{N-1}_{V_U} + 2 \times E^{N-1}_{V_O} - 3 \times E^N + \mu_{UO_2} \quad (5)$$

μ_U and μ_O indicate the chemical potentials of U and O atoms, respectively. The U and O chemical potentials are related at equilibrium by

$$\mu_U + 2\mu_O = \mu_{UO_2} \quad (6)$$

where μ_{UO_2} is obtained from the cohesive energy per UO_2 unitcell [24,25]. Using the thermodynamic relation between oxygen Frenkel and Schottky defects, the formation energies of the vacancies considered as trap sites in UO_2 are derived as shown [13–15]

$$E^f_{V_O} = \frac{1}{2} E^f_{F_O} \quad (7)$$

$$E^f_{V_U} = E^f_S - E^f_{F_O} \quad (8)$$

$$E^f_{V_{UO}} = E^f_S - \frac{1}{2} E^f_{F_O} - E^b_{V_{UO}} \quad (9)$$

$$E^f_{V_{UO_2}} = E^f_S - E^b_{V_{UO_2}} \quad (10)$$

We apply to these relations to the formation energy of $V_{U_2O_2}$ as shown below:

$$E^f_{V_{UO_2}} = E^f_S + \frac{1}{2} E^f_{F_O} - E^b_{V_{U_2O_2}} \quad (11)$$

The movement of vacancies and Xe is investigated by calculating their migration energies. The corresponding energy barrier is obtained at saddle points in their diffusion pathways (See Fig. 3). All the energy values were obtained using the VASP code [26–28]. The PAW method is employed to describe the electron-ion interaction. For the exchange and correlation energy of electrons, we have adopted the conventional GGA approach, because first-principles calculations to the GGA approximation showed that it can give almost correct energy information for UO_2, regardless of the fact that a wrong electronic band structure was predicted [29–32]. Plane waves with a kinetic energy up to 500 eV were used to expand the wave functions, and the electron charge density was obtained by using a $2 \times 2 \times 2$ k-point grid within the Brillouin zone. For all the defect structures, ionic relaxation was performed, and the force acting on each ion was calculated until less than 0.01 eV/Å. Meanwhile, it should be noted that the energy calculations were done by assuming 0 K in this study, even though the movement of point defects can occur at least over 500–600 °C in UO_2. A thermal vibration of the lattice atoms can increase the total energy of a system by about 0.1 eV on average when the system temperature is raised to 1000 °C. However, in this study, the energy value of 0.1 eV could be considered an acceptable error, because the energy change

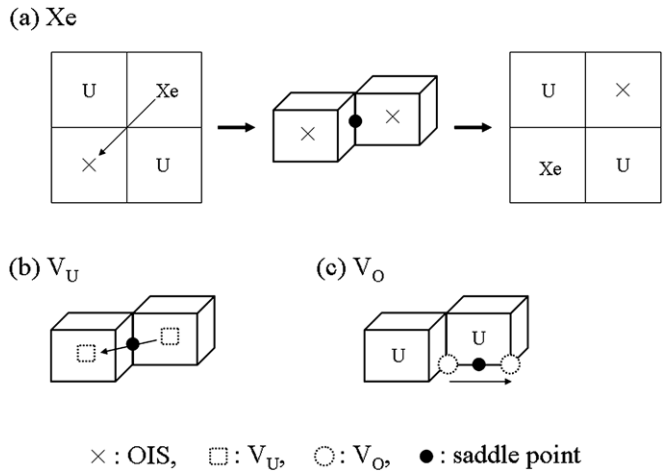

Fig. 3. Diffusion pathways of defect elements between their adjacent lattices sites. The black circles in (a), (b), and (c) indicate the saddle points in the energy pathways of Xe, V_U, and V_O, respectively.

between a perfect crystal and a defect structure was obtained to be about 1–5 eV. We also note that the DFT method has been used successfully to describe numerous materials properties at finite temperatures, despite the limitation of an absolute-zero temperature calculation.

3. Results and discussion

3.1. Stability of Xe

Table 1 shows the calculated incorporation energy of Xe trapped at the five different vacancies. The incorporation energy for an OIS, $E^{I}_{Xe_{OIS}}$, was calculated by using Eq. (1), while $E_{Xe_{free}}$ was obtained from a cubic cell of 10 Å × 10 Å × 10 Å. In Table 1, the positive value of $E^{I}_{Xe_{OIS}}$ indicates that a free Xe atom is more stable than Xe_{OIS} in UO_2. As mentioned in the previous section, we focus on the comparison of the site stability between OIS and vacancies using the relative incorporation energies of Xe. The negative value for the incorporation energy in Table 1 indicates that the energy is decreased when Xe moves from an OIS to vacancies, and then the results show that Xe becomes more stable when it is trapped at a vacancy than at an OIS. Furthermore, Table 1 shows that a larger vacancy is more stable for Xe. It may be closely associated with the size of Xe compared to the host ions in UO_2 (Xe=2.15 Å, U^{4+}=1.01Å, O^{2-}=1.40 Å) [7]. However, if the thermal creation energy of a vacancy is considered as well as the incorporation energy, the majority site of Xe may be a V_{UO} with the lowest value for the sum of incorporation and vacancy formation energy (−5.00 eV) as shown in Table 1. As described in the previous chapter, the vacancy formation energies were determined from the thermodynamic relations [13–15]. We assume that the considered vacancies pre-exist in UO_2. In principle, predominant defects depend on the stoichiometry of UO_2, but the irradiation environment continuously produces point defects on the oxygen and uranium sub-lattices [33]. Therefore, the existence of the vacancy clusters like V_{UO}, V_{UO_2}, and $V_{U_2}O_2$ can be assumed, even though they are not created by thermal activation due to their high formation energies.

The calculated incorporation energies in Table 1 imply that Xe is more likely to be located at a vacancy cluster than at a single vacancy in UO_2. Meanwhile, because of the high incorporation energies, it will be very difficult for Xe to escape from Xe_{UO}, Xe_{UO_2}, and $Xe_{U_2O_2}$, so we suggest an alternative dissociation process. We predict that a single vacancy is separated from a Xe-vacancy complex, and these are calculated the binding energy of a single V_O at Xe-vacancy complexes and summarized in Table 2.

The lowest binding energy of a V_O to Xe_{UO_2} is 1.39 eV. This implies that Xe_{UO_2} is the most unstable among three Xe-vacancy complexes shown in Table 2 and a V_O is more likely to separate from Xe_{UO_2} than other Xe-vacancy complex. From the dissociation of V_O, Xe can be provided a subsequent diffusion pathway. In this study, the separation of a V_U in Xe-vacancy complexes was ignored because of its much higher binding energy compared to those of V_O.

3.2. Vacancy movement

As we mentioned earlier, we concentrate on vacancy-assisted diffusion of Xe. This is because Xe is expected to diffuse by the vacancy mechanism in UO_2, not the interstitial one. This is shown from our calculated result where the energy barrier required for Xe to jump to the saddle point between two OIS is 5.29 eV, see Fig. 3. This relatively-high energy implies that the Xe movement via the interstitial mechanism seems improbable. It was also presented in a previous study [11]. To understand the vacancy-assisted diffusion mechanism of Xe, first we investigated the movement of vacancies. We then calculated the migration energies of a single V_O and V_U and obtained the energy barriers of 1.24 eV for V_O and 4.43 eV for a V_U, respectively, between their two adjacent lattice sites as shown in Fig. 3. The calculated energy barriers of V_O and V_U at the saddle point were overestimated when compared to the experimental data of 0.5 eV and 2.4 eV, respectively [7]. Even though the diffusion process of point defect is very complicated in compound materials and a certain amount of error is taken into consideration, the energy difference in this case is too large to be accepted.

We investigate the origin of this discrepancy and find that it is mainly caused by the spin-restricted calculations. Much improved results were obtained by performing the spin-polarization calculations for antiferromagnetic UO_2 in the [100] directions [24,25], as summarized in Table 3. The energy barrier of Xe_{OIS} is also reduced compared to that obtained from non-magnetic calculations. However, the energy value of 4.48 eV is still too high to take place the interstitial mechanism. This major improvement of the computed energies lead by magnetic exchange interaction has already been presented [35].

For the incorporation and formation energies, relative values of vacancies are more important to understand the stability of trap sites than absolute values. In addition, the non-magnetically

Table 2
Binding energy is needed to separate V_O from an Xe-vacancy complex

Xe-vacancy complexes	Product	Product	Binding energy
Xe_{UO}	Xe_U	V_O	3.27
Xe_{UO_2}	Xe_{UO}	V_O	1.39
$Xe_{U_2O_2}$	Xe_{UO_2}	V_O	2.74

The lowest energy value is obtained at an Xe_{UO_2} among three kinds of Xe-vacancy complexes.

Table 3
Migration energies of single vacancies and Xe_{OIS} obtained from non-magnetism and spin-polarization calculations

Elements	Non-magnetism	Spin-polarization	Experiment [7]
V_O	1.24	0.63	0.5
V_U	4.43	3.09	2.4
V_{UO}	3.24	2.19	–
Xe_{OIS}	5.29	4.48	3.90

calculated formation energies of oxygen Frenkel and Schottky defects agree well with experimental data.

We now consider effective movement of vacancy clusters and find that the migration energy of V_U in the effective movement of V_{UO} was calculated to be 2.19 eV which is lower by about 1.0 eV than the energy obtained without V_O, as shown in Fig. 4.

This result is very comparable with the experimental data of 2.4 eV and suggests that the migration of V_U is likely to take place via the effective movement of vacancy clusters such as V_{UO} in UO_2. Meanwhile, we note that the present study is restricted to neutral defects. The effectively charged vacancy may be important when discussing the atomic transport and energetic calculations. Unfortunately, dealing with charge state of vacancy is beyond a conventional DFT method such as the LDA or GGA, and there is no *ab initio* calculated results using an advanced DFT method so far. However, the energy differences between the different charge states of the vacancies should be very small and negligible compared to the differences between the energies of different kind of defects [36].

3.3. Vacancy-assisted mechanism

In this section, we report the behavior of Xe at various vacancies, in order to understand the vacancy-assisted diffusion mechanism of Xe. From the ionic relaxations, we found that the barrierless movements of Xe occur between two adjacent vacancies because of the strain energy. Fig. 5(a) and (b) show a V_O created at the first nearest lattice site of Xe_U and Xe_{UO}, and then the spontaneous Xe movement take place to the center of the new configuration by about 2 Å.

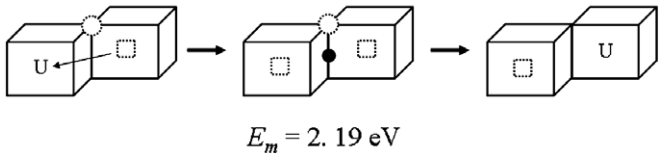

Fig. 4. Migration of V_U in an effective movement of V_{UO}. The corresponding energy barrier of V_U is calculated to be 2.19 eV.

In addition, we found that the strain energy of Xe contributes to the clustering of vacancies in UO_2. Fig. 5(c) and (d) show vacancy-clustering processes when a V_O is created at the second nearest oxygen site of Xe_U or Xe_{UO}. The nearest oxygen atom of Xe_U and Xe_{UO} are pushed towards the created V_O during the ionic relaxations, and Xe_{UO} and Xe_{UO_2} are consequently formed, respectively. However, in Fig. 5(d), the oxygen atom which is taken out of the lattice site cannot reach up to the V_O and finally locates at an interstitial site about 0.78 Å away. Furthermore, the strain energy of Xe is decreased as the trap size is increased and becomes small enough at V_{UO_2} to not affect the displacement of oxygen lattice atom.

By summarizing all the results, we suggest a diffusion process of Xe by the vacancy-assisted mechanism as shown in Fig. 6. On the assumption that Xe is trapped at V_{UO_2}, each step can be described as follows: (1) Xe is moved to the center of the new configuration by the strain energy after a V_O is separated from an Xe_{UO_2}, (2) a new V_O is created at the nearest lattice site of Xe, (3) through the effective movement of a V_U with the help of the new V_O, a configuration of V_{UO_2} is formed again, (4) Xe moves to the center of the V_{UO_2} by the strain energy, (5) and a V_U moves out this configuration.

Considering both of energetic and kinematic properties of V_{UO_2}, we suggest that V_{UO_2} plays a major role in the vacancy-assisted diffusion of Xe in UO_2. V_{UO_2} has not only relatively high incorporation of Xe compared to single vacancies, but also its electrical charge neutrality induced by the same stoichiometric composition with UO_2 is expected to be stable for Xe which is one of inert gases. The formation energy of V_{UO_2} is too large to be created by the thermal activation. However, we find that V_{UO_2} can be created from the vacancy-clustering process by the strain energy of Xe. In addition, it has been known that neutral V_{UO_2} is the simplest and most dominant vacancy cluster among the irradiation-induced defects [7]. Furthermore, Xe_{UO_2} is more unstable than other Xe-vacancy complexes and likely to split with Xe_{UO} and V_O, because of its lower binding energy. This dissociation process provides a subsequent diffusion pathway with Xe. Through these clustering and

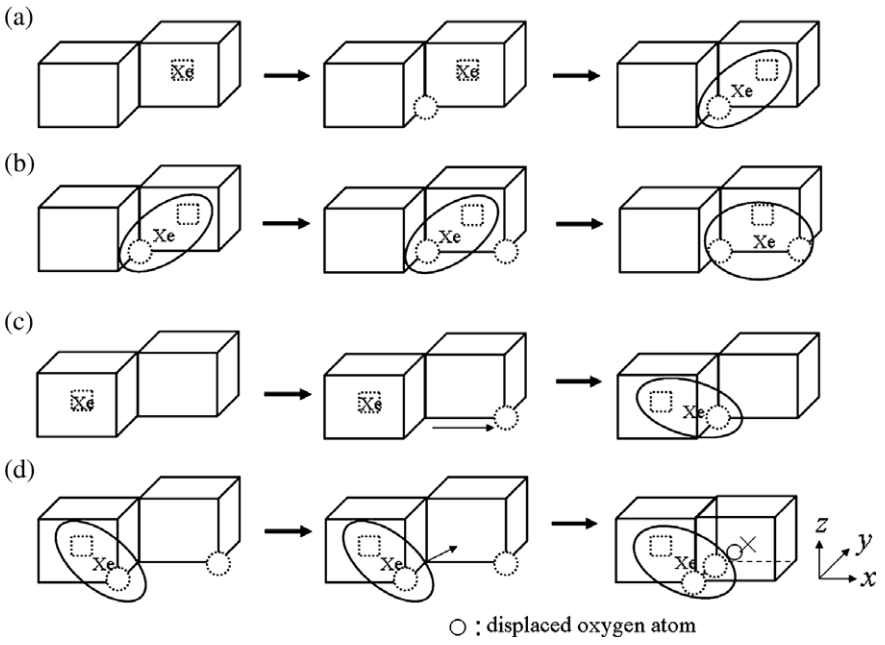

Fig. 5. The vacancy-clustering processes and the barrier-less movement of Xe by the strain energy. (a) and (b): a V_O is formed at the first nearest lattice site of Xe_U and Xe_{UO}, respectively, and Xe moves spontaneously to the center of the new configurations during ionic relaxations. (c) and (d): a V_O is formed at the second nearest lattice site of Xe_U and Xe_{UO}, and then the nearest oxygen atom of Xe is taken out of its lattice site and pushed towards the V_O. Finally, Xe_{UO} and Xe_{UO_2} are formed respectively. However, the displaced oxygen atom in (d) can not reach the V_O site and locates at an interstitial site about 0.78 Å away.

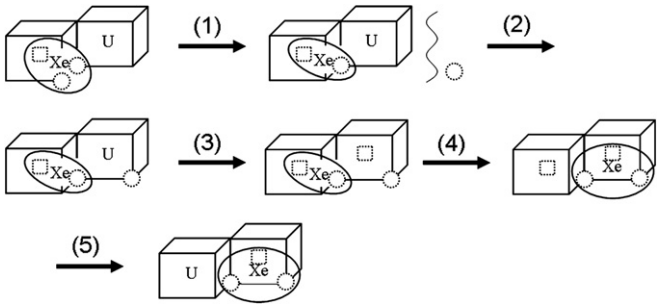

Fig. 6. A possible diffusion pathway of Xe by the vacancy-assisted mechanism in UO_2: (1) a V_O is separated from an Xe_{UO_2}, and Xe moves spontaneously to the center of the new configuration, (2) a new V_O is created at the nearest lattice site of Xe, (3) through the effective movement of a V_U with the help of the new V_O, a configuration of V_{UO_2} is formed again, (4) Xe moves to the center of the V_{UO_2} by the strain energy, (5) and a V_U moves out this configuration.

de-clustering processes of Xe_{UO_2}, the Xe is able to move consecutively in UO_2. We expect that this vacancy-assisted mechanism could explain the experimental data reported by Matzke et al, in that Xe diffusion proceeds via an electrically neutral trivacancy in UO_2[6–8]. In this study, in order to model all the defect structures, we have used a 96-atom supercell while previously a 12 or 24-atom supercell has been used because of computational limitations [17,20,21,33,36]. The influence of the cell size has been discussed as insignificant and the difference of the defect energy between a 12 and 24-atom supercell was 0.05 eV [36]. However, in using periodic boundary conditions, we feel that a $2 \times 1 \times 1$ supercell containing 24 atoms is not enough to ignore the defect-defect interaction. A $2 \times 2 \times 2$ supercell used in this study may still not give an exact energy value, but we stress that the calculation accuracy is improved by reducing the defect-defect interaction. In addition the calculated formation and migration energies of vacancies show a good agreement with the corresponding experimental values as shown in Tables 1 and 3. Thus the 96-atom supercell is a reasonable choice.

4. Conclusion

We have investigated the vacancy-assisted diffusion mechanism of Xe in UO_2, by performing PAW-GGA calculations. In summary, we present two important findings: (1) V_O not only actively hops around in UO_2 due to its low migration energy but also enhances the movement of V_U by leading the effective movement of vacancy clusters; (2) the large strain energy of Xe contributes in creating vacancy clusters and is an important driving force for barrier-less diffusion of Xe in UO_2. In conclusion, we predict a specific diffusion process of Xe via the vacancy-assisted diffusion mechanism. Furthermore, we suggest that a neutral V_{UO_2} is a major diffusion pathway of Xe, because V_{UO_2} is energetically very stable to incorporate Xe, while the Xe_{UO_2} complex is kinetically very unstable to provide Xe with a diffusion pathway. In addition, V_{UO_2} can be created not only by the strain energy of Xe but also by radiation damage. Although there have been some restrictive calculations in this study, we believe the current theoretical simulations contribute strongly to analyzing experimental data microscopically. It also predicts possible fission gas behavior in other nuclear fuel materials such as mixed oxide, and thorium oxide, etc.

Acknowledgements

We gratefully acknowledge discussions with P.M. Oppeneer, L. Werme, and P. Panchmatia. Computer time granted by the Swedish National Infrastructure for Computing (SNIC) is acknowledged. This work was supported by the Korea Research Foundation Grant funded by the Korean Government (MOEHRD) (KRF-2007-35-D00283).

References

[1] J.C. Carter, E.J. Driscoll, T.S. Elleman, Phys. Status Solidi A 14 (1972) 673.
[2] Hj. Matzke, J. Nucl. Appl. 2 (1966) 131.
[3] J.R. MacEwan, W.H. Stevens, J. Nucl. Mater. 11 (1964) 77.
[4] K. Une, I. Tanabe, M. Oguma, J. Nucl. Mater. 150 (1987) 93.
[5] G.T. Lawrence, J. Nucl. Mater. 71 (1978) 195.
[6] Hj. Matzke, J.A. Davies, J. Appl. Phys. 38 (1967) 805.
[7] Hj. Matzke, R.P. Agarwala (Eds.), Diffusion Processes in Nuclear Materials, North Holland, 1992.
[8] Hj. Matzke, Radiat. Eff. 53 (1980) 219.
[9] G. Sattonnay, L. Vincent, F. Garrido, L. Thome, J. Nucl. Mater. 355 (2006) 131.
[10] L. Desgranges, M. Ripert, J.P. Piron, H. Kodja, J.P. Gallier, J. Nucl. Mater. 321 (2003) 324.
[11] C.R.A. Catlow, Proc. R. Soc. Lond. A. 364 (1978) 473.
[12] R.A. Jackson, A.D. Murray, J.H. Harding, C.R.A. Catlow, Philos. Mag. A 53 (2) (1986) 7.
[13] R.W. Grimes, C.R.A. Catlow, J. Am. Ceram. Soc. 72 (1989) 1856.
[14] R.G. Ball, R.W. Grimes, J. Chem. Soc. Farday Trans. 86 (1990) 1257.
[15] R.W. Grimes, C.R.A. Catlow, Philos. Trans. R. Soc. Lond. A 335 (1991) 609.
[16] W. Kohn, L.J. Sham, Phys. Rev. B 13 (1965) 140.
[17] T. Petit, G. Jomard, C. Lemaignan, B. Bigot, A. Pasturel, J. Nucl. Mater. 275 (1999) 119.
[18] O.K. Anderson, Phys. Rev. B 12 (1975) 3060.
[19] H.L. Skriver, The LMTO Method, Springer, Berlin, 1984.
[20] J-P. Crocombette, J. Nucl. Mater. 305 (2002) 29.
[21] M. Freyss, N. Vergnet, T. Petit, J. Nucl. Mater. 352 (2006) 144.
[22] J.P. Perdew, J.A. Chevary, S.H. Vosko, K.A. Jackson, M.R. Pederson, D.J. Singh, C. Fiolhais, Phys. Rev. B 46 (1992) 6671;
J.P. Perdew, J.A. Chevary, S.H. Vosko, K.A. Jackson, M.R. Pederson, D.J. Singh, C. Fiolhais, Phys. Rev. B 48 (1993) 4978E.
[23] G. Kresse, D. Joubert, Phys. Rev. B 59 (1999) 1758.
[24] Y. Yun, Hanchul Kim, Heemoon Kim, K. Park, Nucl. Eng. Tech. 37 (2005) 293.
[25] Y. Yun, H. Kim, H. Lim, K. Park, J. Korean Phys. 50 (2007) 1285.
[26] G. Kresse, J. Hafner, Phys. Rev. B 47 (1993) 588;
G. Kresse, J. Hafner, Phys. Rev. B 49 (1994) 14251.
[27] G. Kresse, J. Furthmüller, Comput. Mat. Sci. 6 (1996) 15.
[28] G. Kresse, J. Furthmüller, Phys. Rev. B 54 (1996) 11169.
[29] H.Y. Geng, Y. Chen, Y. Kaneta, M. Kinoshita, Phys. Rev. B 75 (2007) 054111.
[30] K.N. Kudin, G.E. Scuseria, R.L. Martin, Phys. Rev. Lett. 89 (2002) 266402.
[31] C.J. Pickard, B. Winkler, R.K. Chen, M.C. Payne, M.H. Lee, J.S. Lin, J.A. White, V. Milman, D. Vanderbilt, Phys. Rev. Lett. 85 (2000) 5122.
[32] M. Freyss, T. Petit, J.P. Crocombette, J. Nucl. Mater. 347 (2005) 44.
[33] T. Petit, C. Lemaignan, F. Jollet, B. Bigot, A. Phaturel, Philos. Mag. B 77 (1998) 779.
[34] Hj. Matzke, J. Chem. Soc. Farad. Trans. 2 83 (1987) 1121.
[35] G. Robert, A. Pasturel, B. Siberchicot, Europhys. Lett. 71 (2005) 412.
[36] J.P. Crocombette, F. Jollet, L. Thien Nga, T. Petit, Phys. Rev. B 64 (2001) 104107.